

# Lifetime of heavy hypernuclei and its implications on the weak $\Lambda N$ interaction

W. Cassing<sup>1</sup>, L. Jarczyk<sup>2</sup>, B. Kamys<sup>2</sup>, P.Kulesza<sup>3,4</sup>, H. Ohm<sup>3</sup>, K. Pysz<sup>3,4</sup>, Z. Rudy<sup>2,3</sup>, O.W.B. Schult<sup>3</sup>, and H. Ströher<sup>3</sup>

<sup>1</sup> Institut für Theoretische Physik, Justus Liebig Universität Giessen, D-35392 Giessen, Germany

<sup>2</sup> M. Smoluchowski Institute of Physics, Jagellonian University, PL-30059 Cracow, Poland

<sup>3</sup> Institut für Kernphysik, Forschungszentrum Jülich, D-52425 Jülich, Germany

<sup>4</sup> H. Niewodniczański Institute of Nuclear Physics, PL-31342 Cracow, Poland

Received: date / Revised version: date

**Abstract.** The lifetime of the  $\Lambda$ -hyperon in heavy hypernuclei – as measured by the COSY-13 Collaboration in proton – Au, Bi and U collisions at COSY-Jülich – has been analyzed to yield  $\tau_\Lambda = (145 \pm 11)$  ps. This value for  $\tau_\Lambda$  is compatible with the lifetime extracted from antiproton annihilation on Bi and U targets, however, much more accurate. Theoretical models based on the meson exchange picture and assuming the validity of the phenomenological  $\Delta I=1/2$  rule predict the lifetime of heavy hypernuclei to be significantly larger (2 – 3 standard deviations). Such large differences may indicate that the assumptions of these models are not fulfilled. A much better reproduction of the lifetimes of heavy hypernuclei is achieved in the phase space model, if the  $\Delta I=1/2$  rule is discarded in the nonmesonic  $\Lambda$  decay.

**PACS.** 13.30.-a Decays of baryons – 13.75.Ev Hyperon-nucleon interaction – 21.80 Hypernuclei – 25.80.Pw Hyperon-induced reactions

## 1 Introduction

The  $\Lambda$  hyperon decay can be studied for free hyperons as well as for hyperons colliding with nucleons inside the nuclear medium. In the first case it proceeds via the mesonic

process,  $\Lambda \rightarrow \pi + N$ , with an energy release of about 38 MeV, whereas collisions with nucleons lead to the non-mesonic decay, *e.g.*  $N + \Lambda \rightarrow N + N$ , with an energy release of ( $\sim 180$  MeV).

The mesonic decay also occurs for hyperons bound in hypernuclei, but it is strongly inhibited for all but the lightest hypernuclei due to Pauli blocking of the nucleon final states. The nonmesonic decay, on the other hand, can be studied only in hypernuclei because neither  $\Lambda$  hyperon beams nor targets are available. Due to the immense difficulty in producing  $\Lambda$  hypernuclei and of subsequently detecting their decay the available experimental data on the nonmesonic process are scarce and have large uncertainties.

Most of the measurements for the decay of hypernuclei have been based on limited statistics and been predominantly performed for light hypernuclei (see *e.g.* the reviews [1,2,3] or refs. [4,5,6,7,8,50,10]). Even the total decay rate (or inverse lifetime) of heavy hypernuclei was up to very recently known only with a large error [11]. The experimental knowledge of the partial decay rates is also not satisfactory, *e.g.* the experimental studies devoted to light ( $A \leq 28$ ) [4,5,6,7,10] and medium heavy ( $40 < A < 100$ ) hypernuclei [12,13,14] report different values for the neutron and proton induced  $\Gamma_n/\Gamma_p$  decay rates. The results for light hypernuclei are close to unity whereas those for heavy hypernuclei vary between 1.5 and 9.0. The experimental situation – together with uncertainties in the theoretical description – show that the nonmesonic process is barely understood so far.

We recall that in the Standard Model the weak  $|\Delta S|=1$  transitions can proceed with both  $\Delta I = 1/2$  and  $\Delta I = 3/2$  amplitudes. However, it was found experimentally (in the decays of free kaons and hyperons) that the  $\Delta I = 1/2$

amplitudes dominate by far the  $|\Delta S|=1$  non-leptonic weak interactions [15]. This suppression of the  $\Delta I = 3/2$  amplitude was explained by Miura – Minamikawa [16] and Pati – Woo [17] in terms of the colour symmetry of the valence quarks in the baryon. Thus, one is tempted to assume a dominance of  $\Delta I = 1/2$  transitions also in the nonmesonic decay of the  $\Lambda$  - hyperon. It was, however, observed that theoretical calculations involving this assumption – i.e. only  $\Delta I = 1/2$  transitions – systematically underpredict the ratio  $\Gamma_n/\Gamma_p$  of nonmesonic decay rates induced by neutrons ( $n + \Lambda \rightarrow n + n$ ) to the decay rates induced by protons ( $p + \Lambda \rightarrow p + n$ ) [18]. Several attempts have been made to reconcile this discrepancy *e.g.* in Refs. [19,20,21,22,23,24], but none of them has solved this problem in a convincing way.

This leads to the conclusion that the contribution of the  $\Delta I = 3/2$  transition to the nonmesonic decay of the  $\Lambda$  hyperon might not be negligible, *i.e.* the  $\Delta I = 1/2$  rule should be violated [25,26,27,28,29]. The arguments presented in favor of this hypothesis in refs. [25,26,27,29] have been based essentially on the observed nonmesonic decay widths of the lightest hypernuclei. However, the experimental uncertainties are too large to allow for any definite conclusion. It is thus necessary to get information on the (possible) violation of the  $\Delta I = 1/2$  rule from other properties of hypernuclei, *e.g.* from the mass dependence of the lifetime of hypernuclei as addressed in ref. [28].

As far as experiments are concerned it can be stated from the inspection of Table 1, that the data - with exception of the experiment performed with an  $e^-$  beam

in Kharkov [30] - agree within the limits of errors. In ref. [32] it has been shown, that a hypernucleus fraction decaying on a timescale of 2700 ps (as quoted in [30]) must be smaller by orders of magnitude compared to the fraction of hypernuclei decaying on timescales of 200 ps. However, the errors for  $\tau_\Lambda$  in the measurements from [31, 11] are so large, that no severe constraints could be imposed on the various theoretical models for the nonmesonic decay.

**Table 1.** The lifetimes of heavy hypernuclei from  $e^-$  and  $\bar{p}$  induced reactions from refs. [30,31,11]. The numbers given in parenthesis represent the systematic errors.

Target & projectile	$\tau_\Lambda$ / ps	Ref.	Comment
Bi + e	$2700 \pm 500$	[30]	
Bi + $\bar{p}$	$250^{+250}_{-100}$	[31]	
Bi + $\bar{p}$	$180 \pm 40 (\pm 60)$	[11]	Reanalysis of data from [31]
U + $\bar{p}$	$130 \pm 30 (\pm 30)$	[11]	

In order to improve the situation, experiments with  $Au$ ,  $Bi$  and  $U$  targets have been performed during the last years at the Forschungszentrum Jülich using the internal proton beam of the COSY accelerator by the COSY-13 Collaboration. We briefly describe the different stages of the proton-nucleus reactions – leading to hypernucleus formation and their delayed fission due to the  $\Lambda N \rightarrow NN$  decay – in section 2. The experimental setup used to distinguish prompt and delayed fission events is sketched in section 3 and an overview of the experimental results for

the  $\Lambda$  lifetime is given in section 4. In section 5 we discuss the implication of the latter results for the selection rule  $\Delta I = 1/2$  in the  $\Lambda N \rightarrow NN$  transition. A discussion of open problems and a summary are presented in sections 6 and 7, respectively.

## 2 Heavy hypernuclei formation in $p + A$ reactions and their decays

In case of heavy hypernuclei the application of direct timing methods - as adopted for light hypernuclei - is not feasible due to the large background of light particles produced. This problem is circumvented by detecting heavy fragments from the fission processes, which are induced by the  $\Lambda$ -hyperon decay in heavy hypernuclei. The technique used is the recoil shadow method originally suggested by Metag et al. for the measurement of fission isomers [33]. It has also been employed by Armstrong et al. [11] in the lifetime measurements with antiprotons.

A novel approach to produce heavy hypernuclei for lifetime measurements – as performed by the COSY-13 Collaboration – is to use proton collisions on heavy targets like  $U$ ,  $Bi$  or  $Au$ . The possibility to vary the beam energy allows to measure the background (at a low beam energy, e.g. of 1 GeV) concurrently with the effect (e.g. at 1.9 GeV) by operating COSY in a supercycle, which has not been possible in the  $\bar{p}$  induced reactions in [11]. Furthermore, a variation of the projectile energy in proton induced reactions permits to find out whether an ordinary fission isomer might fake the decay of a hypernucleus. Such

a test is also not possible in antiproton–nucleus interactions since the center-of-mass energy is fixed for stopped antiprotons and always above threshold for  $\Lambda$  production. Furthermore, in  $p + A$  reactions a large part of the proton momentum is transferred to the hypernucleus such that the surviving hypernuclei move faster than in  $\bar{p}$  induced reactions; this increases the sensitivity of the recoil shadow method for lifetime measurements accordingly.

For illustration we show in Fig. 1 the various stages and time scales involved in the  $p + A$  reaction from i) the initial configuration to ii) the associated hyperon production in the target nucleus by  $pN$  inelastic scattering ( $\sim 10^{-23}s$ ), iii)  $\Lambda$  hyperon capture in the residual nucleus via elastic  $\Lambda N$  scattering ( $\sim 10^{-22}s$ ), iv) the  $\Lambda N \rightarrow NN$  reaction on the time scale of  $200\text{ ps}$  leading to v) delayed fission of the hypernucleus. The right part shows the nucleon potentials during the various phases.

Due to the complexity of these reactions the various stages illustrated in Fig. 1 have been simulated by coupled-channel Boltzmann-Uehling-Uhlenbeck (CBUU) transport calculations for the fast nonequilibrium phase [34,35,36,37] followed by Hauser-Feshbach calculations for the statistical evaporation phase [38]. The transport model employed has been used for a variety of hadron-nucleus and nucleus-nucleus reactions from low to relativistic bombarding energies and been tested with respect to the overall reaction dynamics as well as the production of strange and nonstrange hadrons (for reviews see refs. [39,40]). The CBUU calculations provide information on i) the formation cross section of 'hot' hypernuclei as well as on ii)

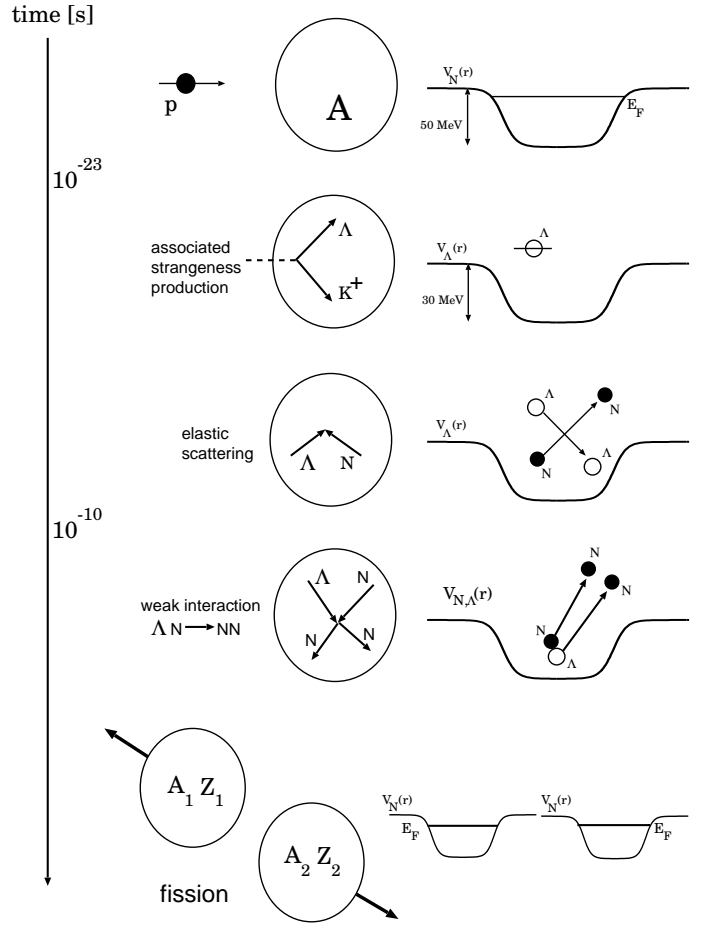


**Fig. 1.** Time evolution of a proton-nucleus collision from i) the initial configuration up to v) the delayed fission of a hypernucleus: ii) associated strangeness production; iii) elastic  $\Lambda N$  scattering; iv) decay of a  $\Lambda$  hyperon via the  $\Lambda N \rightarrow NN$  process leading v) to fission of the excited nucleus. The right part shows the nucleon potentials during the various phases.

the properties of the hypernuclei produced – i.e. primary mass, charge, excitation energy, linear momentum, angular momentum etc. – in a given reaction. The latter information from the CBUU calculation then is used to evaluate (within Hauser-Feshbach calculations) for each event the subsequent statistical decay as well as the probability  $P_s$  of a heavy hypernucleus to survive in competition with prompt fission [37]. Thus, the final distribution in

mass and charge of the 'cold' hypernuclei – reached after  $\sim 10^{-18}s$  (see below) – is evaluated together with their individual ( $A, Z$  dependent) velocity distribution in the laboratory frame. The probability for delayed fission  $P_{f_\Lambda}$  – as induced by the  $\Lambda N \rightarrow NN$  reaction for a hyperon from the  $S$ -state in the individual hypernuclei on a timescale of 200  $ps$  – is calculated again within the Hauser-Feshbach formalism [37]. The kinematics of the fission fragments, furthermore, is simulated according to the Viola systematics [41] assuming isotropic angular distributions for the fission fragments in the rest frame of the decaying hypernucleus. For details we refer the reader to refs. [36,37,42].

The cross sections for  $Au, Bi,$  and  $U$  targets at  $T_{lab} = 1.9$  GeV – as calculated from the CBUU + evaporation calculations – are displayed in Fig. 2, where we show the predicted cross sections and branching ratios for all targets. The experimental cross sections quoted in Fig. 2 for prompt fission have been taken from refs. [43,44]. In contrast to the large differences in the prompt fission cross sections, which amount to a factor of  $\sim 15$  for  $U$  and  $Au$  targets, the cross sections for delayed fission ( $\sim 42, 25$  and  $16 \mu b$  for  $U, Bi$  and  $Au,$  respectively) are rather similar. This is due to the fact that the probability to observe the delayed fission of hypernuclei is determined by a product of two probabilities: the survival probability  $P_s$  of ('hot') hypernuclei against prompt fission and the probability  $P_{f_\Lambda}$  for fission of ('cold') hypernuclei induced by a  $\Lambda$  - hyperon decay. These two probabilities correspond to opposite processes; their sum is approximately equal

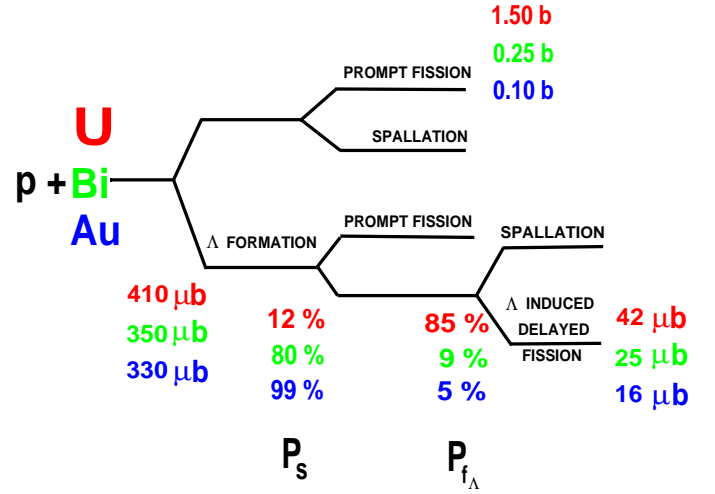


**Fig. 2.** Schematic representation of contributions from different competing processes in p+Au, p+Bi, p+U reactions at  $T_p=1.9$  GeV according to the CBUU + Hauser-Feshbach calculations (see text). The experimental cross sections for prompt fission have been taken from Refs. [43,44].

to unity. We find, furthermore, that also their product remains constant within a factor of 2–3.

The comparison of the cross sections for delayed fission of hypernuclei and prompt fission of target nuclei in Fig. 2 shows that in experiments with  $Bi$  and  $Au$  targets the same statistics for delayed fission fragments can be obtained using 2 – 3 times the beam time for a corresponding uranium experiment. On the other hand, the background from prompt fission in the  $Bi$  or  $Au$  experiments is much smaller because the ratio of the prompt to the delayed fission cross sections is small compared to a  $U$  target. This reduces the load on the detectors in the prompt fission region for  $Au$  and  $Bi$  targets by about an order of magnitude relative to  $U$ . These expectations (calculations) were confirmed in the actual experiments at COSY-Jülich us-

ing *Bi* [32], *Au* [45] and *U* targets [46], where similar cross sections could be observed experimentally.

Another important ingredient for the data analysis (to be discussed later) is the velocity distribution of the hypernuclei in the laboratory. The latter is dominantly determined by the nucleon-nucleon and hyperon-nucleon cross section in the initial stage of the reaction as modeled by the CBUU approach. It has been shown in comparison to independent experimental data from refs. [47,48] that the momentum transfer to the residual nucleus is well described by the transport approach in  $p + U$  reactions for  $T_{lab} = 0.5 - 3$  GeV [46].

During the statistical decay phase the hypernucleus velocity distributions change only moderately, however, a very pronounced change in the mass and charge distributions is observed [37]. The final charges and masses of 'cold' hypernuclei are correlated to form a valley of stability. The resulting two-dimensional spectra in charge  $Z$  and mass  $A$  of cold hypernuclei (typically after  $10^{-18}$  s) are shown in fig. 3 in terms of cluster plots. These differential distributions represent CBUU + evaporation model calculations for hypernuclei produced in the reactions  $p + ^{197}\text{Au}$  at  $T_p=1.7$  GeV,  $p + ^{209}\text{Bi}$  at  $T_p=1.9$  GeV,  $p + ^{238}\text{U}$  at  $T_p=1.9$  GeV. It is seen that the two dimensional plots are quite similar for the three reactions considered, but shifted in mass and charge according to the initial target. It should be noted, that the width of the distribution in charge  $Z$  remains rather constant as a function of mass  $A$ . This can be inferred directly from the isospin-independent emission of protons and neutrons in the pre-

equilibrium CBUU collision stage before the Coulomb barrier is formed; after that the proton emission is suppressed by the Coulomb barrier and neutron emission fills out the 'valley of stability'.

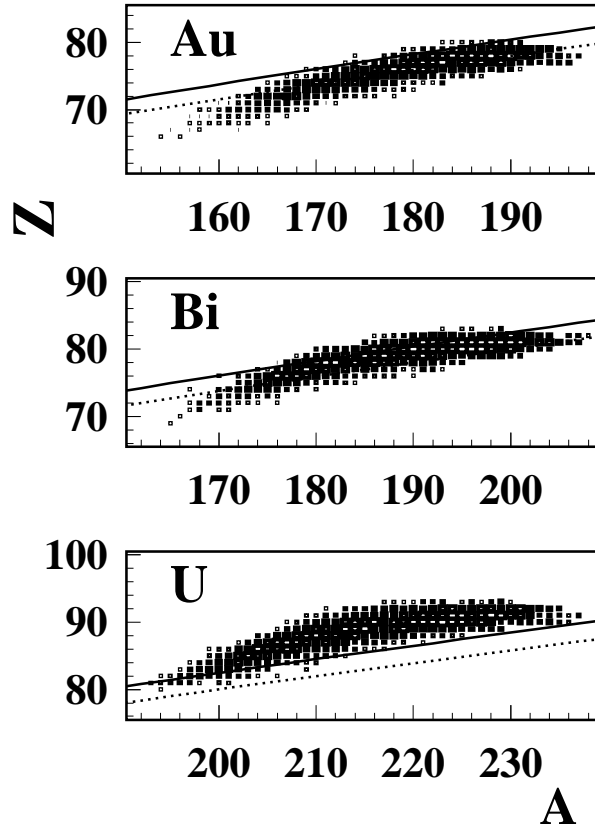


**Fig. 3.** Two dimensional spectra from CBUU + evaporation calculations in charge  $Z$  and mass  $A$  of hypernuclei for  $p + ^{197}\text{Au}$  at  $T_p=1.7$  GeV,  $p + ^{209}\text{Bi}$  at  $T_p=1.9$  GeV and  $p + ^{238}\text{U}$  at  $T_p=1.9$  GeV. The solid and dashed lines indicate hypernuclei of fissility  $Z^2/A = 34$  and  $32$ , respectively. Delayed fission events essentially stem from nuclei with fissility parameter  $Z^2/A \geq 34$ .

It has to be pointed out that although the distributions in mass differ by about 10 to 30 units for the different targets, they have some common overlap region in

the tails. Furthermore, the  $\Lambda$  induced fission probability essentially depends on the fissility parameter  $Z^2/A$  (see Fig.3). The solid and dotted lines in Fig. 3 show hypernuclei of  $Z^2/A = 34$  and  $32$ , respectively. We recall that only a fraction of the  $(A, Z)$  distributions of hypernuclei created in  $p + A$  interactions lead to actual delayed fission events (see  $P_{f\Lambda}$  in Fig. 2), i.e. essentially for  $Z^2/A \geq 34$ . When averaging over the experimental results for all targets one thus obtains a value for  $\tau_\Lambda$  that corresponds to an average over all nuclei with masses  $A \geq 180$ .

### 3 Experimental setup and data analysis

Hypernuclei produced in proton-nucleus collisions, which survive the prompt fission stage, leave the target with a recoil velocity  $v_R$ . They subsequently decay at some distance from the target proportional to the lifetime  $\tau_\Lambda$  of the  $\Lambda$ -hyperon and to the velocity  $v_R$ . Thus prompt and delayed fission events can be separated by the spatial distribution of their decays. The problem, however, is that the prompt fission events are more frequent than the delayed fission processes by factors of  $\sim 10^5$  (cf. Fig. 2) – which corresponds to the ratio of prompt to delayed fission cross sections – and the spatial distribution of delayed events has to be measured with high accuracy. The particular solution to this problem is provided by the recoil shadow method [33], which allows to analyse the spatial distribution of delayed decays with respect to the product  $\tau_\Lambda \cdot v_R$  in the presence of a huge background compared to the investigated effect.

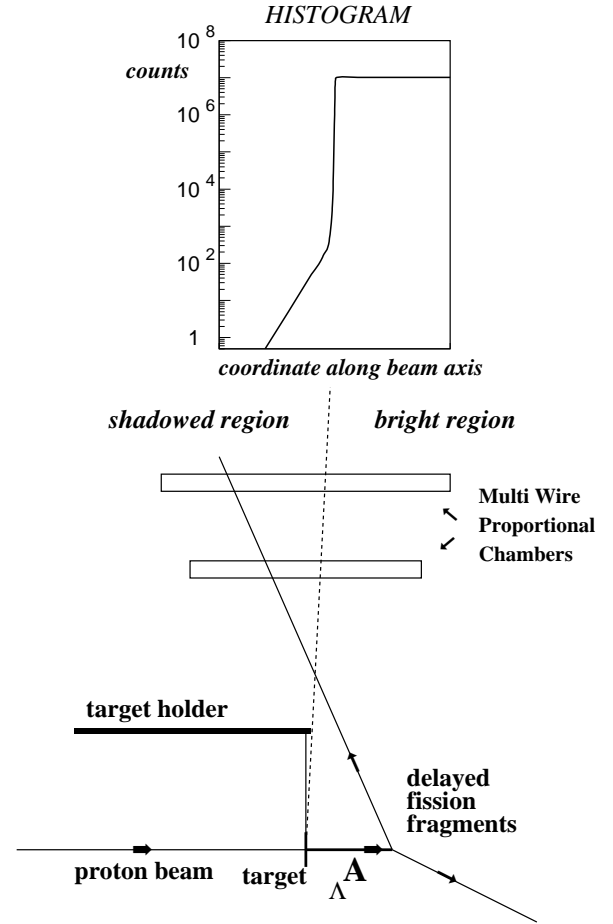


**Fig. 4.** Schematic view of the experimental setup and illustration of the recoil distance method (see text). The dimension of the target holder and target in the lower part are increased by a factor  $\approx 30$  relative to the MWPC's.

A schematic view of the detection scheme [49] is shown in Fig. 4, where the dimensions of the target and its holder – serving as a diaphragm – are increased by a factor  $\approx 30$  in comparison to the dimensions of the low pressure multiwire proportional chambers (MWPC) placed 30 cm from the target in a direction perpendicular to the target. The multiwire chambers are sensitive to fission fragments, but not sensitive to protons and other lighter particles. These detectors were partly screened by the target holder such

that the prompt fission fragments - originating from the target - could not hit the shadowed (left) part of the detector. This was, however, possible for fragments from the delayed fission of hypernuclei  ${}_{\Lambda}A$  escaping from the target downstream the beam and fissioning in some distance from the target. A schematic event distribution - projected on to the beam axis - is shown in the upper part of Fig. 4, which is characterized by an exponential fall-off for the delayed fission events in the shadowed (left) region and a constant (prompt) yield in the bright (right) region of the detector. For further details we refer the reader to ref. [49].

In order to check whether the events detected in the shadow region are not light particles or even  $\gamma$ 's, the following tests have been performed:

- The MWPC were irradiated with minimum ionizing particles ( $\gamma$ 's and  $e^-$ ); it was shown that the detection efficiency for such particles is below  $10^{-11}$ .
- A pure carbon foil was used as a target in  $p + A$  measurements, leaving the detection system unchanged. The measured spectra in the shadowed part of the detectors were found to contain no events.
- A  ${}^{252}\text{Cf}$  source was placed at the target position and a two-dimensional energy loss versus time-of flight spectrum (between both MWPC) was measured. The spectrum was populated in line with Monte Carlo calculations taking into account the mass, charge and velocity distributions of fragments according to the Viola systematics [41] from the fission of californium.

The fragments, that hit the shadowed (left) part of the detector, thus originate either from the delayed fission of hypernuclei (or hyperfragments) or they are emitted in prompt fission from the target and due to scattering on the shadow edge (part of the target holder) have changed their initial trajectories. Therefore, scattering creates a background in the shadow region with an intensity proportional to the prompt fission cross section. In order to determine the background distribution of hits in the shadowed part of the detector measurements have been performed at a much lower proton energy ( $T_p=1.0$  GeV), where the cross section for hypernucleus production is expected to be negligibly small (about 4 orders of magnitude smaller than at 1.9 GeV), whereas the prompt fission yield is about the same.

It has been shown by Monte Carlo simulations that hyperfragments from prompt fission of hypernuclei, that have changed their direction due to the recoil induced by a subsequent  $\Lambda$ -hyperon decay, can hit the shadowed region of the detectors only in a very narrow region of 1-2 mm close to the edge of the shadow region and, thus, do not contribute to the distribution that was actually used for the extraction of the lifetime of hypernuclei (see below).

The proton beam (with typically  $5 \cdot 10^{10}$  protons in the COSY-ring) has been accelerated up to 1.9 GeV (for the observation of hypernucleus production) and to 1.0 GeV (for an estimation of the background originating from scattered fragments from prompt fission of the target nucleus). The COSY accelerator was operated in the super-cycle mode, *i.e.* there were three cycles (each of  $\sim 15$  s



duration) of beam acceleration and irradiation of the target; two of them at the higher energy of 1.9 GeV and one at 1.0 GeV. This allowed to study the effect and the background concurrently for the same shape and thickness of the target.

The distribution of hit positions of the fission fragments on the surface of the detector then were projected on to the beam direction. The respective distributions for the  $Au$ ,  $Bi$ , and  $U$  target are shown in the upper parts of Figs. 5, 6, 7 at  $T_p = 1.9$  GeV (full dots) together with the background measured at  $T_p = 1.0$  GeV (open circles).

These experimental distributions then have been compared with simulated distributions, which were evaluated assuming the velocity distribution of the hypernuclei (as obtained from the CBUU + Hauser-Feshbach calculations) and a lifetime of the  $\Lambda$ -hyperon in the hypernuclei, where the latter was treated as a free parameter in the fit procedure. Since the number of events in the position distributions was not very large in some experiments, a Poisson instead of Gaussian probability distribution  $p(n_i)$  has been used to simulate the number of counts  $n_i$  for each position bin (cf. ref. [46]). Then the best lifetime  $\tau_\Lambda$  was searched for by the 'maximum likelihood' method, which allows also for an estimate of the statistical error for  $\tau_\Lambda$  (see *e.g.* ref. [50]). The results of the fits are shown in the lower part of Figs. 5, 6, 7 by the solid lines in the shadow region in comparison to the experimental data, where the background (measured at  $T_p = 1.0$  GeV) has been subtracted from the 1.9 GeV data.

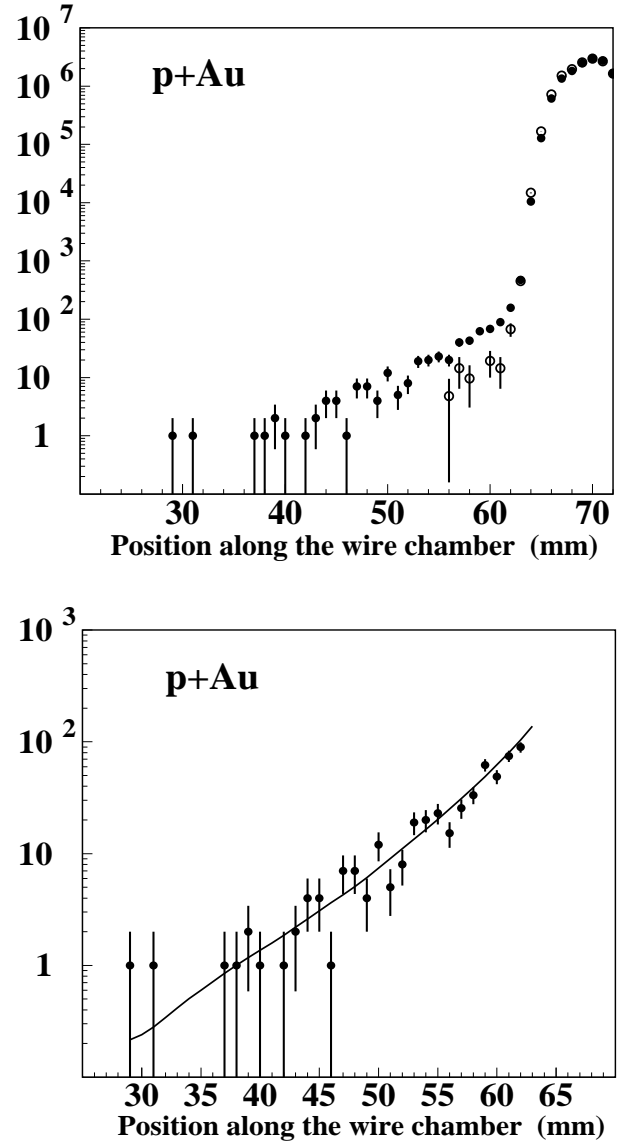


**Fig. 5.** Upper part: The position distribution of hits of fission fragments in the position sensitive detectors for the  $p + Au$  experiment (from ref. [45]). The full dots represent the data for  $T_p=1.9$  GeV whereas the open circles show the data for  $T_p=1.0$  GeV renormalized in the bright part of the detectors to the 1.9 GeV data. Lower part: The position distribution of hits from the delayed fission fragments of hypernuclei in the shadow region obtained by subtracting the background (renormalized data taken at 1.0 GeV) from the data measured at 1.9 GeV. The solid line shows the result of the simulation with the extracted value for the lifetime according to the maximum likelihood method.

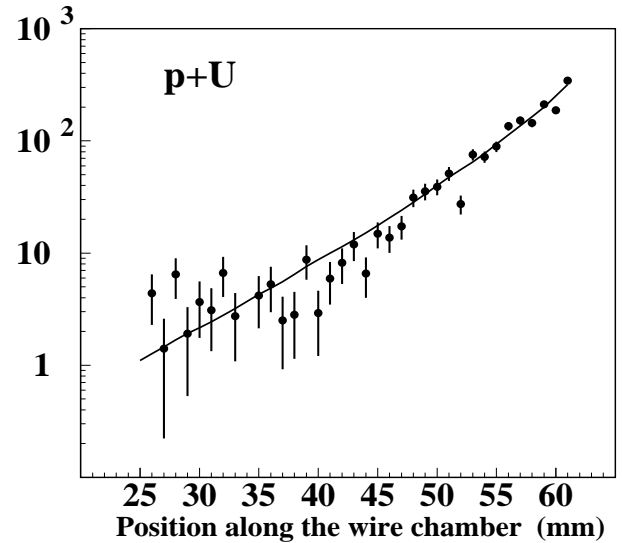
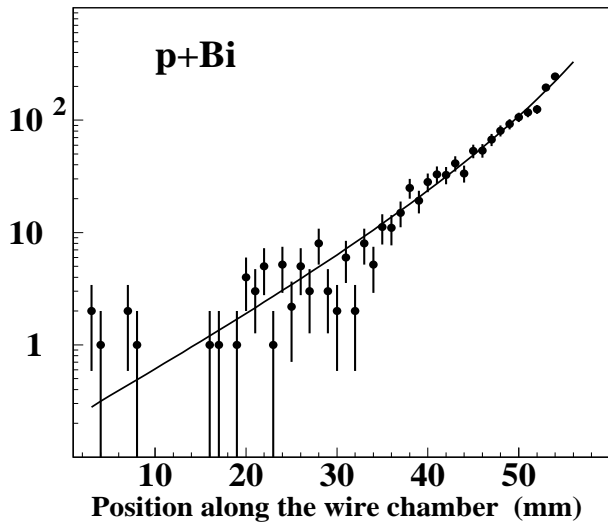
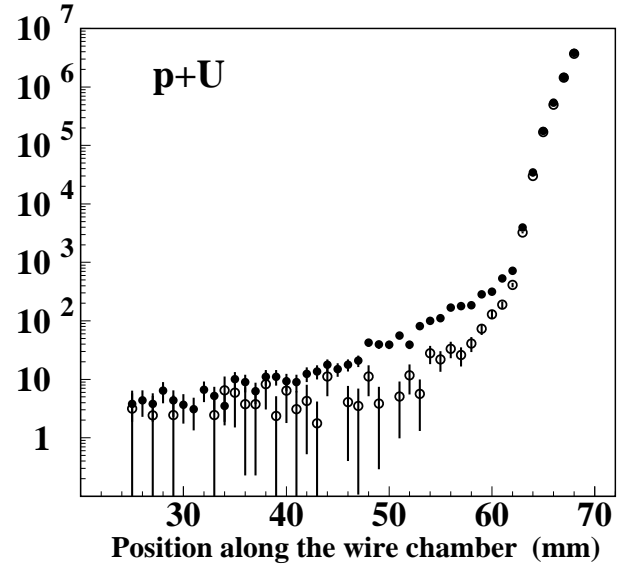
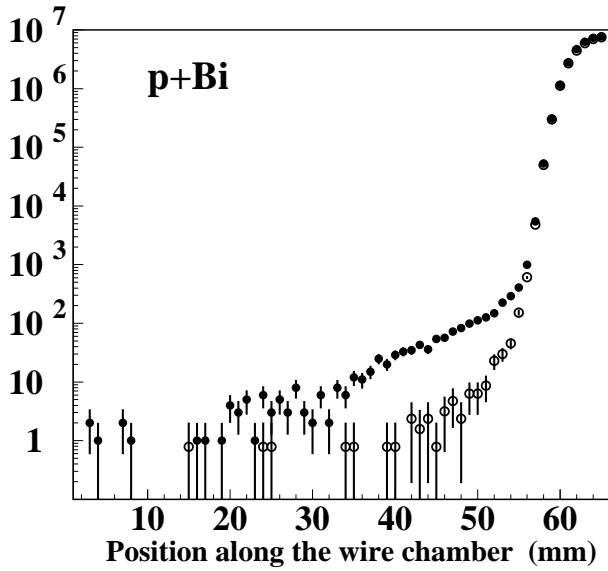


Fig. 6. The same distributions as in Fig. 5 for the  $p + \text{Bi}$  experiment (from ref. [32]).

Fig. 7. The same distributions as in Fig. 5 for the  $p + \text{U}$  experiment (taken from ref. [46]).

The question arises, whether the velocity distributions of hypernuclei might differ significantly when varying  $(A, Z)$ . In such a case the simulation of the position distributions, which is the crucial part in the analysis of the experimental data, should be carried out by folding the velocity distributions of hypernuclei with specified  $(A, Z)$  with the fission time distributions of these hypernuclei. However, as detailed calculations have shown [42], those hypernu-

clei, that lead finally to fission, have practically the same velocity distribution.

#### 4 Summary of experimental results and error analysis

In this section we summarize the results of the COSY-13 Collaboration and compare to the lifetimes measured be-

fore (cf. Table 1). Such a comparison must necessarily involve a discussion of experimental uncertainties. Whereas the *statistical* errors can be unambiguously determined by the maximum likelihood method as described in detail in ref. [46], the estimation of *systematic* errors has to be discussed individually for each experiment, since the number of events in the shadow region of the detectors have been different as well as the stability of the individual targets during the irradiation periods.

#### 4.1 Systematic errors

The systematic errors arise from:

- a.) the velocity distribution of hypernuclei,
- b.) an anisotropic emission of the fission fragments,
- c.) a nonuniform irradiation of the target by the proton beam,
- d.) a change of position and shape of targets during the measurements,
- e.) the background treatment in case of low statistics, and
- f.) the explicit search procedure ( $\chi^2$  or maximum likelihood methods) for the best lifetime.

Detailed simulations have been carried out to determine the variation in the lifetime  $\tau_\Lambda$  according to the error sources listed above. The results of these studies in ref. [46] lead to the actual numbers shown in Table 2 for the three targets separately.

The systematic errors can be summed up to 15 ps for the Au target, to 14 ps for the Bi target, and to 17 ps for the U target.

**Table 2.** The sources of systematic errors in the COSY-13 experiments. The total systematic error has been evaluated assuming that the sign of all contributions is the same.

Source of errors	Au	Bi	U
a.) velocity distribution	2 ps	2 ps	2 ps
b.) anisotropic emission	2 ps	2 ps	2 ps
c.) nonuniform irradiation	4 ps	4 ps	4 ps
d.) change of shape and position	2 ps	1 ps	4 ps
e.) background treatment	3 ps	3 ps	3 ps
f.) search procedure	2 ps	2 ps	2 ps
Total	15 ps	14 ps	17 ps

#### 4.2 Results

We recall that due to the rather large dispersion in the  $(A, Z)$  distribution of cold hypernuclei (cf. Fig. 3) the observation of the delayed fission of these nuclei does not give an information on the lifetime of specific heavy hypernuclei, i.e. with fixed atomic number  $Z$  and mass  $A$ , but it rather provides a lifetime averaged over a group of different hypernuclei.

**Table 3.** The lifetime of heavy hypernuclei measured at COSY-Jülich by COSY-13. The errors in the third column have been obtained by quadratically adding the statistical and systematic errors from the second column.

Target	$\tau_\Lambda$ / ps	$\tau_\Lambda$ / ps	Ref.
Au	$130 \pm 13(\text{stat.}) \pm 15(\text{syst.})$	$130 \pm 20$	[45]
Bi	$161 \pm 7(\text{stat.}) \pm 14(\text{syst.})$	$161 \pm 16$	[32]
U	$138 \pm 6(\text{stat.}) \pm 17(\text{syst.})$	$138 \pm 18$	[46]

A summary for the lifetimes  $\tau_\Lambda$  including the statistical and systematic errors is presented in Table 3. It can be concluded, that the experiments performed with the proton beam on  $Au$ ,  $Bi$ , and  $U$  targets give consistent and comparable values for the lifetime of heavy hypernuclei. Within statistics these values are identical, though the average masses of the fissioning hypernuclei differ for the different targets (cf. Fig. 3). On the other hand, the individual distributions in  $(A, Z)$  overlap such that we may also average over the three experiments to obtain an average lifetime for hypernuclei with masses  $A \approx 180 - 225$  with a dispersion in charge  $\Delta Z \approx 3$  (for fixed  $A$ ) as:

$$\tau_\Lambda = 145 \pm 11 \text{ ps} \quad (\text{for } p+A).$$

### 4.3 Comparison with antiproton induced reactions

This average lifetime of heavy hypernuclei is within the statistical error limits in agreement with the lifetimes extracted from antiproton experiments Refs. [11] (see Table 1), which by averaging over the  $Bi$  and  $U$  targets amounts to:

$$\tau_\Lambda = 143 \pm 36 \text{ ps} \quad (\text{for } \bar{p}+A).$$

In fact, the mass and charge distribution of hypernuclei from the experiments with antiprotons should be similar to those of the proton induced reactions since a comparable energy is transferred to the nucleus. However, the latter reactions lead to a much more precise value for  $\tau_\Lambda$  since i) the background can be determined experimentally in contrast to the  $\bar{p}$  induced reactions - which reduces the systematic errors - and ii) the velocity of the hypernuclei is much larger in the laboratory due to the higher momen-

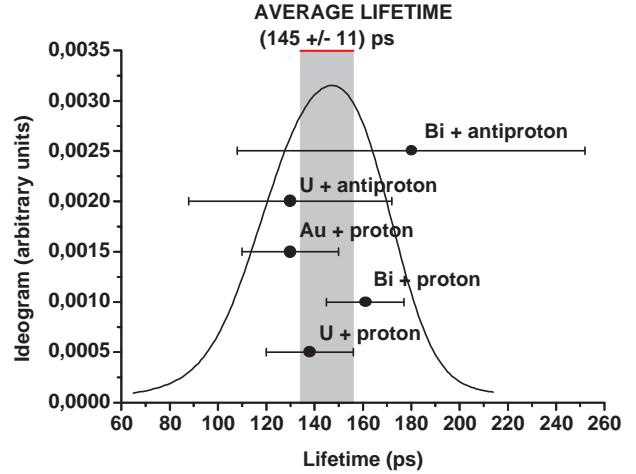


**Fig. 8.** The lifetimes for proton and antiproton produced hypernuclei on  $Au$ ,  $Bi$  and  $U$  targets. The horizontal bars present the statistical and systematic errors added in quadrature. The gray vertical bar displays the overall average value for the lifetime of heavy hypernuclei and its width shows the error. The smooth Gaussian-like curve was evaluated as proposed in the Review of Particle Physics [50], *i.e.* adding Gaussian curves representing results from individual experiments. Parameters of these Gaussian curves (average value and standard deviation) are equal to the individual lifetimes and their errors (square roots from sum of squares of statistical and systematic errors). The weights - with which the individual curves enter the sum - were chosen as reciprocals of the errors quoted above.

tum transfer from the proton at  $T_p = 1.9$  GeV. The latter fact also leads to a cleaner separation of delayed fission events from prompt fission events in the shadowed region of the detector, that stem from small angle scattering in the target holder. Moreover, the geometrical conditions of proton induced reactions allow for a less ambiguous inter-

pretation of fission fragment distributions in the shadowed regions of the detectors than those for antiproton experiments because in the former investigations it was possible to neglect the contribution of hyperfragments which originate from prompt (not delayed) fission of hypernuclei, but are observed in the shadow region due to recoil caused by subsequent decay of the  $\Lambda$ -hyperon.

A compilation of all results discussed above for the lifetime  $\tau_\Lambda$  from proton and antiproton induced reactions is presented in Fig. 8 in the form proposed in the Review of Particle Physics [50]. We note, that adding the result from the  $\bar{p}$  experiments to the data from COSY-13 does not change the number of  $\tau_\Lambda = 145 \pm 11$  ps quoted above.

## 5 Implications for the $\Lambda N \rightarrow NN$ reaction

The dependence of the lifetime on the mass number of the hypernucleus is shown in fig. 9. The experimental results for light hypernuclei (mass number  $11 \leq A \leq 56$ ) seem to be mass independent within the limits of errors. The lifetimes of heavy hypernuclei as measured by the COSY-13 collaboration do not indicate a mass dependence in the studied range of mass numbers ( $180 \leq A \leq 225$ ) either. However, experiments show that the lifetimes of heavy hypernuclei are shorter by  $\sim 60 - 70$  ps than those for light hypernuclei. This difference implies that the lifetime should decrease by less than 0.5 ps per mass unit. Such a weak decrease could not be established within the present experimental accuracy if the light or the heavy hypernuclei are studied separately. In both cases the covered mass range is about 45 mass units corresponding to a variation

of the lifetime by about 20 ps, i.e. less than two experimental errors.

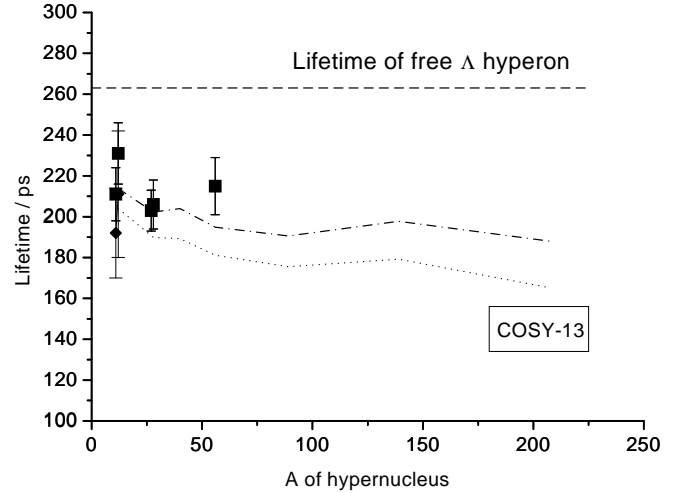


**Fig. 9.** Mass dependence of the  $\Lambda$ -lifetime. Diamonds and squares represent experimental data obtained for light hypernuclei in refs [5,6] and [8,9], respectively. The rectangle placed at  $A \sim 200$  represents the experimental result obtained for heavy hypernuclei by the COSY-13 collaboration. The width of the rectangle indicates the range of masses of the hypernuclei observed in the COSY-13 experiments ( $180 \leq A \leq 225$ ), whereas the height corresponds to the experimental accuracy quoted (11 ps). The dot-dashed line and dotted line present results of theoretical calculations from refs. [51] and [52], respectively, while the horizontal dashed line shows the experimental lifetime of the free  $\Lambda$  hyperon.

The dotted and dot-dashed lines in fig. 9 represent theoretical model expectations evaluated within the meson exchange model. In both calculations the validity of the  $\Delta I = 1/2$  rule has been assumed and the contribution from nonmesonic decays initiated by two nucleons was included. Nevertheless, the results of the calculations differ

rather significantly, i.e.  $\sim 10$  ps for light and  $\sim 20$  ps for heavy hypernuclei.

However, the smooth decrease of the lifetime versus mass of the hypernuclei is a common property of both model calculations, i.e. both approaches reproduce qualitatively the mass dependence of the experimental data as extracted from the comparison of lifetimes of light and heavy hypernuclei. Furthermore, both models predict a weaker decrease of the lifetime with mass than observed in the experiment. The calculations of Alberico et al. [51] lead to a difference between the largest lifetime (for  ${}_{\Lambda}^{12}C$ ) and the smallest one (for  ${}_{\Lambda}^{208}Pb$ ) of about 26 ps. Similarly, this difference in the model of Jido et al. [52] is 39 ps, whereas the difference in the average experimental lifetimes from light and heavy hypernuclei is approximately 60 – 70 ps. Such a large discrepancy between theory and experiment should indicate an inadequacy of one or more model assumptions.

As discussed in the introduction and demonstrated in ref. [28], the  $\Delta I = 1/2$  rule might be violated in the  $\Lambda N \rightarrow NN$  interaction contrary to the case of free hyperon decays. In this respect we recall that the lifetime of heavy hypernuclei is sensitive to the ratio  $R_n/R_p$  of the neutron induced to proton induced  $\Lambda$  nonmesonic decays  $\Lambda + N \rightarrow N + N$ , whereas the lifetime of light hypernuclei ( $A \approx 12$ ) is independent of this ratio. Thus, a precise knowledge of the lifetime of light hypernuclei (which depends only on  $R_n+R_p$ ) and an accurate knowledge of the lifetime of heavy hypernuclei (depending both on  $R_n+R_p$

and on  $R_n/R_p$ ) enables us to determine the absolute normalization, i.e.  $R_n+R_p$ , as well as the ratio  $R_n/R_p$ .

Furthermore, we can test the validity of the phenomenological  $\Delta I = 1/2$  rule due to the following reasons: The ratio  $R_n/R_p$  vanishes for final state isospin  $I_f=0$  since the neutron induced  $\Lambda$  decay leads only to neutron-neutron final states, which cannot form an isospin zero state. On the other hand, the ratio  $R_n/R_p$  is equal 2 for  $\Delta I = 1/2$  decays to pure  $I_f=1$  final states (realized e.g. for  $\Lambda$  - nucleon spin state  $S$ ) [27]. Therefore, in the general situation - where the observed decays correspond to an incoherent mixture of the  $I_f=0$  and  $I_f=1$  final states - pure  $\Delta I = 1/2$  decays must always result in a ratio  $R_n/R_p \leq 2$ . Any measured ratio  $R_n/R_p \geq 2$  then will indicate a violation of this rule. We will argue in the following that this should be indeed the case.

To sharpen the arguments we show again the theoretical calculations from ref. [28] for the  $\Lambda$  hyperon lifetime for both, the mesonic and nonmesonic contributions included, in Fig. 10 as a function of the hypernucleus mass  $A$ . In these calculations the strength of the weak transition  $\Lambda N \rightarrow NN \sim R_n + R_p$  is fixed in magnitude to the data (cf Fig. 10) for light hypernuclei with  $N \approx Z$  and masses  $A \approx 12$ . We mention that this strength has an error of about 5% according to a statistical analysis of the lifetimes for these nuclei which amounts to  $\approx \pm 7$  ps for heavy hypernuclei ( $A \sim 200$ ).

The calculations for a constant ratio  $R_n/R_p$  then lead to a smooth decrease for the lifetime as a function of mass  $A$  which approximately saturates for  $A \approx 160$  (solid line

for  $R_n/R_p=1$ ). When increasing the ratio to  $R_n/R_p = 2$  we obtain the dashed line which is the lowest limit for the  $\Delta I = 1/2$  rule to hold according to the argumentation presented above. Any further increase of  $R_n/R_p$  (dotted line) leads to a steeper dependence of  $\tau_\Lambda$  with mass  $A$  since in neutron rich nuclei – along the line of stability – the  $n\Lambda \rightarrow nn$  channel becomes the dominant one.

When comparing the different theoretical lines with the lifetime extracted from the present work for masses  $A \geq 180$  (hatched area with COSY-13), we find that a ratio  $R_n/R_p \leq 2$  is not compatible with  $\tau_\Lambda = 145 \pm 11$  ps for the heavy hypernuclei. Thus within the described scenario the  $\Delta I=1/2$  rule is violated.

The latter conclusion also holds, when the contribution of two nucleon induced decays ( $\Lambda+n+p \rightarrow n+n+p$ ) is taken into account since it was shown by Ramos et al. [21], that the yield of two nucleon induced decays of  $\Lambda$  hyperons is independent of the mass of the hypernucleus. The presence of such a mass-independent contribution effects the mass dependence of lifetimes in the same way as a decrease of the  $R_n/R_p$  ratio, i.e. it makes the mass dependence less steep. Therefore, an experimental indication for a steeper mass dependence relative to the theoretical result for the one nucleon induced decay – under the assumption of the validity of the  $\Delta I = 1/2$  rule – becomes an even stronger argument for a violation of this rule when two nucleon induced decays contribute.

Since this conclusion is based on experimental data for lifetimes of light and heavy hypernuclei, which are biased by statistical and systematic errors, the violation of the  $\Delta I$

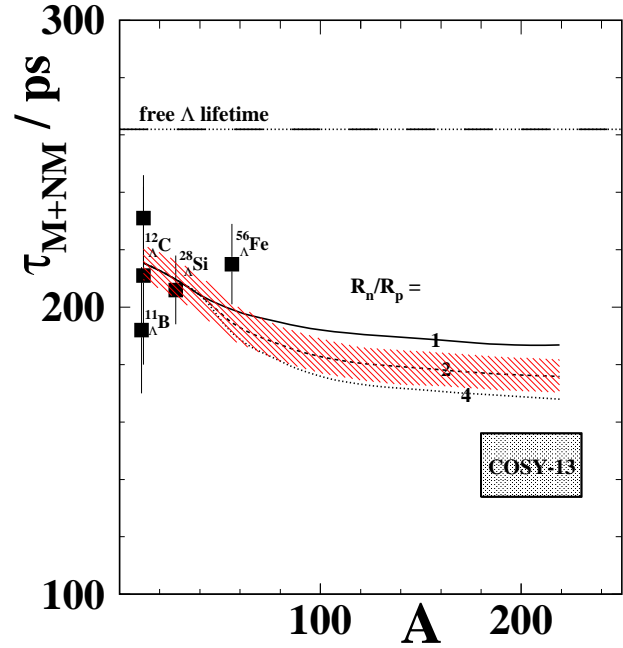


**Fig. 10.** Calculations of the  $\Lambda$ -lifetime  $\tau_{M+NM}$  due to the mesonic and nonmesonic decay as a function of the hypernucleus mass  $A$  in the valley of stability (from ref. [28]) in comparison to the data of Refs. [8,6]. The COSY-13 collaboration result for nuclei with masses  $A \geq 180$  is marked by the hatched area labelled "COSY-13". The width and height of this rectangle represent the range of hypernucleus masses involved and the error of the lifetime determination, respectively. In the theoretical calculations both mesonic and non-mesonic decay modes are taken into account whereas the unknown ratio of the weak decay rates  $R_n/R_p$  is treated as a parameter with values:  $R_n/R_p = 1,2,4$ . The hatched area around the dashed line (corresponding to  $R_n/R_p=2$ ) shows the  $\pm\sigma$  uncertainty in the magnitude of the weak transition  $\sim (R_n + R_p)$  determined from the lifetimes of light hypernuclei with  $A \approx 12$ .

$= 1/2$  rule can only be stated with some confidence level  $P_c < 1$ . To estimate this probability we followed the error analysis described in Ref. [28] using the present average value for the lifetime of heavy hypernuclei (cf. fig. 10) with

the error evaluated as a sum of statistical and systematic errors (11 ps). This leads to a confidence level  $\approx 0.98$ ; an inclusion of the antiproton data from ref. [11] (Table 1) does not modify this result.

It should be emphasized, that the mass dependence of the lifetime varies only weakly with the ratio  $R_n/R_p$  for large values of this ratio. Thus the error in the normalization of the theoretical curves in fig. 10, *i.e.*  $\pm 7$  ps – the error of  $R_n/R_p$  determined by the accuracy of the lifetimes of light hypernuclei – and the error of the lifetime for heavy hypernuclei, *i.e.*  $\pm 11$  ps (as extracted from the COSY-13 data) do not allow to establish the ratio  $R_n/R_p$  more precisely; it can only be stated that it is larger than 2.

## 6 Discussion

The conclusions presented above rely on: i) the accuracy of the overall normalization, which is a free parameter of the present theoretical model, and ii) the assumption that the model predictions with respect to the mass dependence of the hypernuclei lifetimes are reliable. We will discuss these premises in the following.

We recall that the theoretical model formulated in ref. [28] is based on the transport Boltzmann-Uehling-Uhlenbeck equation (BUU). It treats the nuclei as systems of fermions in a selfconsistent mean field with mutual in-medium interactions allowed by the Pauli principle. Due to the semiclassical limits invoked the approach neglects the shell structure of the nuclei.

The decay width of the nonmesonic decay is evaluated from the collision rate of hyperons with nucleons in the target using local Thomas-Fermi distributions for the nucleon phase-space density and a 1s state wavefunction for the hyperon. Since the cross section for the  $\Lambda+N \rightarrow N+N$  weak process is not known from experiment, it was assumed in ref. [28] that the differential cross section for the weak  $\Lambda+N \rightarrow N+N$  process is proportional to the cross section of elastic  $\Lambda+N \rightarrow \Lambda+N$  scattering. This is the most far-reaching approximation of this model, which may influence both, the normalization of the mass dependence of  $\tau_\Lambda$  and the shape of this mass dependence.

ad i) The absolute normalization – a free parameter of the model – is responsible for all mass independent factors. It has been determined from a comparison of the experimental and theoretical results for light hypernuclei, where our model results do not depend on the ratio  $R_n/R_p$ . In detail: The normalization has been performed to an average value of the lifetimes for  ${}^1_1\text{B}$  and  ${}^{12}_\Lambda\text{C}$  [50, 8, 6]. Within this normalization the confidence level for a violation of the  $\Delta I=1/2$  rule is found to be  $\sim 0.98$ . Taking the experimental lifetimes for  ${}^{12}_\Lambda\text{C}$  and for  ${}^1_1\text{B}$  [50, 6] separately gives confidence levels of 0.99 and 0.95 for a normalization to  ${}^{12}_\Lambda\text{C}$  and to  ${}^1_1\text{B}$ , respectively. This shows, that the uncertainty in the normalization cannot change the conclusion concerning the violation of the  $\Delta I=1/2$  rule.

ad ii) However, as mentioned above, the lack of knowledge of the elementary cross section for the weak  $\Lambda+N \rightarrow N+N$  process might influence the shape of the mass dependence of  $\tau_\Lambda$ .



To check the sensitivity of  $\tau_\Lambda$  on the elementary cross section for the weak  $\Lambda+N \rightarrow N+N$  process the calculations have been performed also with a constant (energy independent) cross section and compared with the results of ref. [28]. It was found that the mass dependence for the energy independent cross section turned out to be even flatter in mass  $A$  and the lifetimes for heavy hypernuclei increased by  $\sim 13$  ps. Such a limit increases the difference between the experimental lifetime of heavy hypernuclei and the theoretical model and thus more strongly supports a violation of the  $\Delta I=1/2$  rule.

Furthermore, to explore the least favorable situation for rejecting the validity of the  $\Delta I=1/2$  rule, i.e. assuming a much steeper mass dependence, we have evaluated the confidence level for the case, where the limiting curve for  $R_n/R_p=2$  is shifted downwards by 20 ps for heavy hypernuclei. Even for such a significant modification of the model the confidence level is still quite large,  $\sim 0.75$ , in favor of a violation of the  $\Delta I=1/2$  rule.

To gain further insight into the validity of our theoretical model we have, furthermore, compared the mass dependence of the hypernucleus lifetime from ref. [28] with the mass dependence from the more recent calculations of W. M. Alberico et al. [51] and D. Jido et al. [52]. Since in both studies the validity of the  $\Delta I=1/2$  rule has been assumed, we compare the mass dependence from ref. [28] within the same assumption (i.e. the limiting value  $R_n/R_p=2$  has been adopted) and omitted the contribution of two-nucleon induced  $\Lambda$ -hyperon decays in the re-

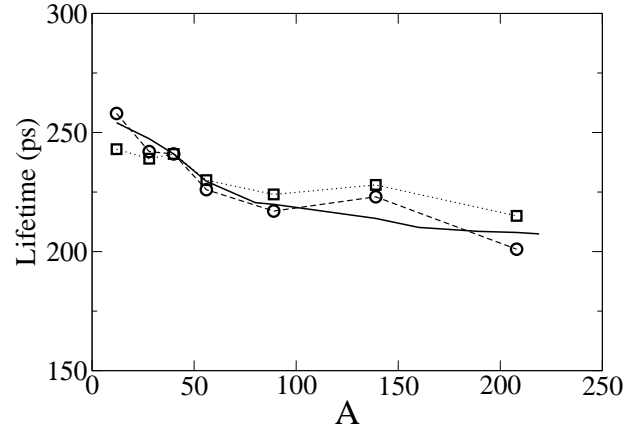


**Fig. 11.** Mass dependence of the  $\Lambda$ -lifetime  $\tau_{M+NM} = 1/(\Gamma_M + \Gamma_1)$  due to the mesonic and nonmesonic decay induced by single nucleons – as evaluated in refs. [51] (squares) and [52] (circles) – in comparison with the mass dependence calculated in ref. [28] for  $R_n/R_p=2$  and normalized to each other at  $A=40$ .

sults of refs. [51] and [52], since the model of ref. [28] does not include this contribution.

The calculated results for the mass dependence of  $\tau_\Lambda$  from these three models are presented in Fig. 11, where the squares correspond to the calculations of ref. [51], the circles to the calculations of ref. [52] while the solid line shows the mass dependence from ref. [28] after normalization to the lifetime of  ${}^{40}_\Lambda\text{Ca}$ , which is predicted by the two other studies to be exactly the same. The agreement of the mass dependence from ref. [28] with the results of the two other works is quite remarkable. In our opinion this points towards a satisfactory reliability of the phase-space model [28].

We thus conclude, that in spite of the uncertainty in the shape as well as the uncertainty in the overall normalization of the theoretical mass dependence of  $\tau_\Lambda(A)$

the experimental lifetime from COSY-13 is small enough to derive valid conclusions concerning a violation of the  $\Delta I=1/2$  rule.

Our conclusions – which specify that the ratio of neutron induced to proton induced weak decays of the  $\Lambda$  hyperons in heavy hypernuclei is larger than 2 – should be confronted with available results obtained from experiments, where the ratio  $\Gamma_n/\Gamma_p$  was measured by a straightforward detection of nucleons from the decay of hypernuclei. These results are shown in table 4.

The data for heavy hypernuclei on this ratio have been obtained in refs. [12,13,14] by using photographic emulsions to observe the decays of heavy hypernuclei in the mass range 40 – 100. An analysis of the energy spectra of fast protons was used for this purpose. In all these works a dominance of neutron induced over proton induced decays has been reported with a  $\Gamma_n/\Gamma_p$  ratio in the range from 1.5 to 9.0, which is in line with our findings.

On the other hand, a much smaller ratio of  $\Gamma_n/\Gamma_p$  ( $\sim 1$ ) has been observed for light hypernuclei, where also spectra of fast protons have been analysed. Here e.g. the results by J.J. Szymanski et al. [6] for  ${}^5_{\Lambda}He$ ,  ${}^{11}_{\Lambda}B$  and  ${}^{12}_{\Lambda}C$  are smaller than 2; this is also in line with the recent measurements of O. Hashimoto et al. [10] for  ${}^{12}_{\Lambda}C$  and  ${}^{28}_{\Lambda}Si$ .

The experimental situation thus appears to create a puzzle;  $\Gamma_n/\Gamma_p$  is found to be larger than 2 for heavy hypernuclei whereas it is apparently close to unity for light hypernuclei. Thus, either the analysis of the experiments

**Table 4.** The ratios of decay widths  $\Gamma_n/\Gamma_p$  for light and heavy hypernuclei obtained from a straightforward detection of fast protons from the nonmesonic decay of the  $\Lambda$  hyperon

Hypernucleus or range of masses of hypernuclei	$\Gamma_n/\Gamma_p$	Ref.
$40 < A < 100$	1.5 – 9.0	[12]
$40 < A < 100$	9.0	[13]
$A \sim 50$	$\sim 5$	[14]
${}^{28}_{\Lambda}Si$	$1.38^{+0.13+0.27}_{-0.11-0.25}$	[10]
${}^{12}_{\Lambda}C$	$1.33^{+1.12}_{-0.81}$	[6]
${}^{12}_{\Lambda}C$	$1.17^{+0.09+0.020}_{-0.08-0.18}$	[10]
${}^{11}_{\Lambda}B$	$1.04^{+0.59}_{-0.48}$	[6]
${}^5_{\Lambda}He$	$0.93 \pm 0.55$	[6]

is biased by some mass-dependent effects, or this ratio is indeed different for light and heavy hypernuclei.

## 7 Summary

In this work we have summarized the experimental studies of the COSY-13 Collaboration that aimed at measuring the lifetime  $\tau_{\Lambda}$  of the  $\Lambda$  hyperon in heavy nuclei produced in proton induced reactions on  $Au$ ,  $Bi$  and  $U$  targets employing the recoil shadow method. The lifetimes extracted from the various experiments are all compatible with each other and also with the lifetimes determined by early antiproton annihilation experiments on  $Bi$  and  $U$  targets from ref. [11], however, much more accurate. These lifetimes correspond to a broad range in mass and charge of the produced hypernuclei (cf. Fig. 3) with a rather narrow dispersion in charge (for fixed A). This mass range is

comparable to the mass range of light hypernuclei studied up to now.

Averaging the lifetime  $\tau_\Lambda$  over all results from the COSY-13 measurements we obtain

$$\tau_\Lambda = 145 \pm 11 \text{ ps.}$$

This value for the lifetime of heavy hypernuclei is smaller than the results of recent theoretical calculations by W.M. Alberico et al. [51] ( $\sim 188$  ps) and D. Jido et al. [52] ( $\sim 165$  ps), which have been performed for the full range of masses of hypernuclei, by more than 3 and 2 standard deviations (in the first and the second case, respectively). In the framework of the theoretical model of ref. [28] such a small value for  $\tau_\Lambda$  may be explained by a dominance of the neutron induced over proton induced decay rates ( $R_n/R_p > 2$ ). This implies that the empirical  $\Delta I = 1/2$  isospin rule – found for the vacuum decays of single strange hadrons and assumed to be valid in the theoretical calculations of W.M. Alberico et al.[51] and D. Jido et al.[52] – is violated for the in-medium  $\Lambda N \rightarrow NN$  transition. The latter reactions involve a high momentum transfer, *i.e.* they test the  $\Lambda N$  weak interaction at short distances, where the overlap of the quark wave functions is very large. It is questionable, if these compact 'parton configurations' might be described properly in the meson-exchange picture based on effective hadronic lagrangians. A description with partonic degrees of freedom, which includes automatically  $\Delta I = 3/2$  transitions, should be more

adequate, but reliable calculations on the partonic level still have to wait for future.

### Acknowledgements

This work has been supported by the DLR International Bureau of the BMBF, Bonn, and the Polish Committee for Scientific Research.

### References

1. J. Cohen, Prog. Part. Nucl. Phys. **25** (1990) 139
2. E. Oset, A. Ramos, Prog. Part. Nucl. Phys. **41** (1998) 191
3. W. M. Alberico and G. Garbarino, e-print archive: nucl-th/0112036
4. A. Montwill, P. Moriarty, D. H. Davis, T. Pniewski, T. Sobczak, O. Adamovic', U. Krecker, G. Coremans - Bertrand, J. Sacton, Nucl. Phys. **A234** (1974) 413,
5. R. Grace, P. D. Barnes, R. A. Eisenstein, G. B. Franklin, C. Maher, R. Reider, J. Seydoux, J. Szymanski, W. Wharton, S. Bart, R. E. Chrien, P. Pile, Y. Xu, R. Hackenburg, E. Hungerford, B. Bassaleck, M. Barlett, E. C. Milner, R. L. Stearns, Phys. Rev. Lett. **55** (1985) 1055
6. J.J. Szymanski, P.D. Barnes, G.E. Diebold, R.A. Eisenstein, G.B. Franklin, R. Grace, D.W. Hertzog, C.J. Maher, B.P. Quinn, R. Rieder, J. Seydoux, W.R. Wharton, S. Bart, R.E. Chrien, P. Pile, R. Sutter, Y. Xu, R. Hackenburg, E.V. Hungerford, T. Kishimoto, L.G. Tang, B. Bassaleck, R.L. Stearns, Phys. Rev. **C43** (1991) 849
7. H. Noumi, S. Ajimura, H. Ejiri, A. Higashi, T. Kishimoto, D.R. Gill, L. Lee, A. Olin, T. Fukuda, O. Hashimoto, Phys. Rev. **C52** (1995) 2936

8. H.C. Bhang, S. Ajimura, K. Aoki, T. Hasegawa, O. Hashimoto, H. Hotchi, Y.D. Kim, T. Kishimoto, K. Maeda, H. Noumi, Y. Ohta, K. Omata, H. Outa, H. Park, Y. Sato, M. Sekimoto, T. Shibata, T. Takahashi, M. Youn, Nucl. Phys. **A639** (1998) 269c
9. H. Park, H. Bhang, M. Youn, O. Hashimoto, K. Maeda, Y. Sato, T. Takahashi, K. Aoki, Y. D. Kim, H. Noumi, K. Omata, H. Outa, M. Sekimoto, T. Shibata, T. Hasegawa, H. Hotchi, Y. Ohta, S. Ajimura, T. Kishimoto, Phys. Rev. **C61** (2000) 054004
10. O. Hashimoto, S. Ajimura, K. Aoki, H. Bhang, T. Hasegawa, H. Hotchi, Y. D. Kim, T. Kishimoto, K. Maeda, H. Noumi, Y. Ohta, K. Omata, H. Outa, H. Park, Y. Sato, M. Sekimoto, T. Shibata, T. Takahashi, and M. Youn, Phys. Rev. Lett. **88** (2002) 042503
11. T.A. Armstrong, J.P. Bocquet, G. Ericsson, T. Johansson, T. Krogulski, R.A. Lewis, F. Malek, E. Monnard, J. Mougey, H. Nifenecker, J. Passaneau, P. Perrin, S.M. Polikanov, M. Rey-Campagnolle, C. Ristori, G.A. Smith, G. Tibell, Phys. Rev. **C47** (1993) 1957
12. J. P. Lagnaux, J. Lemonne, J. Sacton, E. Fletcher, D. O'Sullivan, T. P. Shah, A. Thompson, P. Allen, Sr. M. Heeran, A. Montwill, J. E. Allen, D. H. Davis, D. A. Garbutt, V. A. Bull, P. V. March, M. Yaseen, T. Pniewski, J. Zakrzewski, Nucl. Phys. **60** (1964) 97
13. J. Cuevas, J. Diaz, D. M. Harmsen, W. Just, E. Lohrmann, L. Schink, H. Spitzer, M. W. Teuchner, Nucl. Phys. **B1** (1967) 411
14. S.N. Ganguli and M.S. Swami, Proc. Indian Acad. Sci. **67** (1967) 77
15. J.F. Donoghue, E. Golowich, and B.Holstein, Phys. Rep. **131** (1986) 319
16. K. Miura and T. Minanikawa, Prog. Theor. Phys. **38** (1967) 954
17. J.C. Pati and C.H. Woo, Phys. Rev. **D3** (1971) 2920
18. K. Hagino and A. Parreño, Phys. Rev **C 63** (2001) 044318
19. A. Parreño, A. Ramos, C. Benhold, K. Maltman, Phys. Lett. **B435** (1998) 1
20. W.M. Alberico, A. De Pace, M. Ericson and A. Molinari, Phys. Lett. **B256** (1991)134
21. A. Ramos, M.J. Vicente-Vacas, E.Oset, Phys. Rev. **C55** (1997) 735; Erratum arXiv:nucl-th/0206036 v1
22. J.F. Dubach, G.B. Feldman, B.R. Holstein, L. de la Torre, Ann. Phys. (N.Y.) **249** (1996) 146
23. M.J. Savage and R.P. Springer, Phys. Rev. **C53** (1996) 441; Erratum *ibid.* **54** (1996) 2786
24. K. Sasaki, T. Inoue and M. Oka, Nucl. Phys. **A 669** (2000) 331 ; Erratum Nucl. Phys. **A 678** (2000) 455
25. C.B. Dover, Few-Body Systems Suppl. **2** (1987)
26. J. Cohen, Phys. Rev. **C42** (1990) 2724
27. R.A. Schumacher, Nucl. Phys. **A547** (1992) 143c
28. Z. Rudy, W. Cassing, L. Jarczyk, B. Kamys, P. Kulesa, O.W.B. Schult, A. Strzalkowski, Eur. Phys. J. **A5** (1999) 127
29. W.M. Alberico, G. Garbarino, Phys. Lett. **B 486** (2000) 362
30. V.I. Noga, Yu.N. Ranyuk, N. Ya. Rutkevich, P.V. Sorokin, E.V. Sheptulenko, Sov. J. Nucl. Phys **43** (1986) 856, *ibid.* **46** (1987) 769
31. J.P. Bocquet, M. Epherre-Rey-Campagnolle, G.Ericsson, T. Johansson, J. Mougey, H. Nifenecker, P. Perrin, S. Polikanov, C. Ristori, G. Tibell, Phys. Lett. **B182** (1986) 146, *ibid.* **B192** (1987) 312

32. P. Kulesa, Z. Rudy, M. Hartmann, K. Pysz, B. Kamys, I. Zychor, H. Ohm, L. Jarczyk, A. Strzałkowski, W. Cassing, H. Hodde, W. Borgs, H.R. Koch, R. Maier, D. Prasuhn, M. Motoba, O.W.B. Schult, Phys. Lett. **B427** (1998) 403
33. V. Metag, E. Liukkonen, G. Sletten, O. Glomset, S. Bjornholm, Nucl. Instr. & Meth. **114** (1974) 445
34. Gy. Wolf, G. Batko, W. Cassing, U. Mosel, K. Niita, M. Schäfer, Nucl. Phys. **A517** (1990) 615
35. Gy. Wolf, W. Cassing, U. Mosel, Nucl. Phys. **A552** (1993) 549
36. Z. Rudy, W. Cassing, T. Demski, L. Jarczyk, B. Kamys, P. Kulesa, O.W.B. Schult, A. Strzałkowski, Z. Phys. **A351** (1995) 217
37. Z. Rudy, W. Cassing, T. Demski, L. Jarczyk, B. Kamys, P. Kulesa, O.W.B. Schult, A. Strzałkowski, Z. Phys. **A354** (1996) 445
38. A. Gavron, in 'Computational Nuclear Physics', vol. 2 'Nuclear Reactions', ed. by K. Langanke, J.A. Maruhn and S.E. Koonin, Springer Verlag 1993, p. 108
39. W. Cassing, V. Metag, U. Mosel, K. Niita, Phys. Rep. **180** (1990) 363
40. W. Cassing, E.L. Bratkovskaya, Phys. Rep. **308** (1999) 65
41. V.E. Viola, K. Kwiatkowski, M. Walker, Phys. Rev. **C31** (1985) 1550
42. Z. Rudy, Report INP No 1811/PH, Cracow 1998;  
(<http://mezon.if.uj.edu.pl/~kamys/COSY13/zrhab.pdf>)
43. J. Hudis and S. Katcoff, Phys. Rev. **C13** (1976) 1961
44. L.A. Vaishnane, L.N. Andronenko, G.G. Kovshevny, A.A. Kotov, G.E. Solyakin, W. Neubert, Z. Phys. **A302** (1981) 143
45. B. Kamys, P. Kulesa, H. Ohm, K. Pysz, Z. Rudy, H. Ströher, and W. Cassing, Eur. Phys. J. **A 11** (2001) 1
46. P. Kulesa, W. Cassing, L. Jarczyk, B. Kamys, H. Ohm, K. Pysz, Z. Rudy, H. Ströher, Acta Physica Polonica **B33** (2002) 603
47. Z. Fraenkel, A. Breskin, R. Chechik, S. Wald, R. Abgeg, H.W. Fielding, P. Kitching, S.T. Lam, G.C. Neilson, W.C. Olsen, J. Uegaki, Phys. Rev. **C41** (1990) 1050
48. A.A. Kotov, et al., Sov. J. Nucl. Phys. **17** (1974) 498; *ibid.* **19** (1974) 385
49. K. Pysz, I. Zychor, T. Hermes, M. Hartmann, H. Ohm, P. Kulesa, W. Borgs, H.R. Koch, R. Maier, D. Prasuhn, Z. Rudy, B. Kamys, W. Cassing, J. Pfeiffer, Y. Uozumi, L. Jarczyk, A. Strzałkowski, O.W.B. Schult, Nucl. Instr. & Meth. **A420** (1999) 356
50. Particle Data Group, Eur. Phys. J. **C15** (2000) 1
51. W. M. Alberico, A. De Pace, G. Garbarino, and A. Ramos, Phys. Rev. **C61** (2000) 044314,
52. D. Jido, E. Oset, J. E. Palomar Nucl. Phys. **A694** (2001) 525